Available online at www.sciencedirect.com
SCIENCE DIRECT
Journal of the European Ceramic Society 26 (2006) 469–474
www.elsevier.com/locate/jeurceramsoc

Type-A zeolites with hydroxyapatite surface layers formed by an ion exchange reaction

Yujiro Watanabe [a,*], Toshiyuki Ikoma [b], Yasushi Suetsugu [b], Hirohisa Yamada [c], Kenji Tamura [c], Yu Komatsu [a], Junzo Tanaka [b], Yusuke Moriyoshi [d]

[a] *College of Environmental Engineering and Architecture, Kanazawa Institute of Technology, 7-1 Ohgigaoka, Nonoichi, Ishikawa 921-8501, Japan*
[b] *Biomaterials Center, National Institute for Materials Science, 1-1 Namiki, Tsukuba, Ibaraki 305-0044, Japan*
[c] *Ecomaterials Center, National Institute for Materials Science, 1-1 Namiki, Tsukuba, Ibaraki 305-0044, Japan*
[d] *Faculty of Engineering, Hosei University, 3-7-2 Kajinocho, Koganei, Tokyo 184-8584, Japan*

Available online 10 August 2005

Abstract

To enhance adsorption of harmful ions on type-A zeolites (LTA), hydroxyapatite (HAp) thin layers were synthesized on the LTA surface by an ion exchange reaction of Ca^{2+} for NH_4^+ under hydrothermal treatment. The temperatures and durations in the reactions were varied ranging from 25 to 200 °C and from 1 to 168 h. The samples synthesized were characterized by X-ray diffraction method (XRD), scanning electron microscopy (SEM), transmission electron microscopy (TEM) and Brunauer–Emmet–Teller method (BET). The structure of LTA was not destroyed by the hydrothermal treatments at 25 to 160 °C for 8 h and also at 120 °C for 1 to 72 h. The yield of HAp grown on the LTA surface, synthesized at 120 °C for 8 h, showed a maximum value of 0.82. The morphologies of HAp were dependent mainly on the temperatures. The specific surface area remained unchanged in the treatments at 25 to 40 °C for 8 h, as compared to the specific surface area of Ca-LTA, however up to 80 °C, the value decreased with an increase of exchange temperature.

Keywords: Apatite; Composite; Zeolite; Electron microscopy; Surfaces

1. Introduction

Zeolites consist of a three-dimensional open-framework structure composed of AlO_4 and SiO_4 tetrahedra linked together by oxygen sharing, and contain channels and cavities into which cations and water molecules diffuse, as well as functioning as ion-exchange sites.[1] More than 100 different species of synthetic zeolites have been identified.[2] Linde type A zeolite ($(X_{12/m})(Si_{12}Al_{12}O_{48})\cdot nH_2O$, X = cation, m = charge number, LTA) is the most useful among the zeolites due to highest cation exchange capacity (CEC).[1] LTAs are widely used as an ion exchanger for ammonium and cadmium,[3–6] and are considered to utilize them for the adsorption of radioactive elements, such as cesium and iodine.[7] Hydroxyapatite [$Ca_{10}(PO_4)_6(OH)_2$, HAp] has a high CEC for cadmium and lead, and shows a high stability in an alkaline solution.[8] These properties are suitable for adsorbents or materials to fix harmful elements by controlling the morphology and the amount of HAp on the LTA surface.

Several studies have succeeded in growing apatite crystals on the surfaces of wollastonite and alite for biological and medical applications.[9–12] However, in these studies, the substances are self-destroyed when coating their surfaces with HAp. We have been focused on the preparation of multi-functional ceramic composites with the adsorption and/or fixation properties. In our previous studies, LTA with HAp thin layers were prepared by a hydrothermal treatment at 120 °C for 8 h based on the basis of a cation exchange reaction.[13,14] The hydrothermal treatment did not destroy the cubic automorphism but changed its surface morphology by covering evenly with needle crystals of nano-HAp.

In this study, HAp thin layers were synthesized on the LTA surface by hydrothermal treatment at different tem-

* Corresponding author. Tel.: +81 76 248 9504; fax: +81 76 294 6723.
E-mail address: yujiro@neptune.kanazawa-it.ac.jp (Y. Watanabe).

0955-2219/$ – see front matter © 2005 Elsevier Ltd. All rights reserved.
doi:10.1016/j.jeurceramsoc.2005.07.024

peratures and duration in the reactions. The crystal phases and morphologies of HAp grown on the LTA surface were evaluated by the powder X-ray diffraction method (XRD), scanning electron microscopy (SEM) and transmission electron microscopy (TEM). The yield of HAp was calculated from the weight changes and the amount of Si, Al, Ca and P in samples analyzed by inductivity coupled plasma–atomic emission spectroscopy (ICP-AES) before and after the reactions. The specific surface areas and pore diameters were evaluated by the Brunauer–Emmet–Teller (BET) method.

2. Experimental

2.1. Preparation of LTA with Ca^{2+}

LTA with Ca^{2+} (Ca-LTA) as a starting substance for hydrothermal treatments was prepared as follows. LTA with Na^+ (Na-LTA) was purchased from Wako Pure Chemicals Industries, Ltd. The exchange of Na^+ for Ca^{2+} was carried out by immersing and stirring 5.0 g of the Na-LTA in 1500 ml of a 0.5 M $CaCl_2$ solution for 24 h. The resultant sample was filtered with a membrane filter of 0.45 μm in pore size and rinsed with distilled water to remove excess cations. The Ca-LTA was then dried at 100 °C for 24 h.

2.2. Synthesis of HAp crystals on the LTA surface

Hydrothermal treatments were conducted as follows: 0.3 g of the Ca-LTA powder was immersed in 20 ml of a 1 M $(NH_4)_3PO_4$ solution in a 100 ml Teflon cup fitted into a stainless steal pressure vessel. The pH value was controlled to 9 by the addition of an ammonium solution. The suspension was heated at different temperatures ranging from 25 to 200 °C and duration ranging from 1 to 168 h. The samples were quenched and washed three times with distilled water, and dried at 100 °C for 24 h. The Ca-LTA and the resultant samples after the hydrothermal treatments were investigated by XRD (Rigaku, RINT2200) with monochromatized Cu Kα radiation at 40 kV and 40 mA. The morphology was observed by SEM (Hitachi S-5500) and TEM (Hitachi H-9500 operated at 300 kV). The yield was calculated from the weight changes of samples before and after the reactions. The composition of the samples before and after the reaction at 120 °C was determined by ICP-AES (SEIKO HVR 1700). For the measurement of Si and Al, 50 mg of each sample was fused with Na_2CO_3 (0.5 g) and H_3BO_3 (0.2 g) in a platinum crucible at 1000 °C for 10 min. The mixtures were dissolved in 11.6 mol/l of HCl solution, and distilled water was added to the solutions to the final volume of 100.0 ml. For the measurement of Ca and P, 50 mg of each sample was dissolved in 2 ml of HF (27 M) and 1 ml of H_2SO_4 (18 M), and evaporated. The dried residues were then dissolved in 11.6 mol/l of HCl solution with heating, and distilled water was added to the solutions to the final volume of 100 ml.

2.3. Specific surface areas measurement of LTA with HAp layers

The samples after the hydrothermal treatments were immersed in 1500 ml of a 0.5 M $CaCl_2$ solution for 24 h for the ion exchange of NH_4^+ for Ca^{2+}. The resultant samples were filtered with a membrane filter of 0.45 μm in pore size and rinsed with distilled water to remove excess cations. The samples obtained were dried at 100 °C for 24 h. 0.05 g of the samples and Ca-LTA obtained in Section 2.1 were degassed at 200 °C for 3 h in vacuum. The specific surface areas and pore diameters were measured by the multipoint Brunauer–Emmet–Teller method using a Beckman Coulter SA3100 instrument with N_2 gas as an adsorbent.

3. Results and discussion

Fig. 1 shows the XRD patterns of Ca-LTA before and after the hydrothermal treatment at 120 °C for the durations of 1–168 h. The Ca-LTA exhibited the complete exchange of Na^+ for Ca^{2+} in LTA, which was judged from the change of diffraction intensities and the appearance of a new diffraction at 25.1° in 2θ (Fig. 1a).[15] After the hydrothermal treatment of Ca-LTA at 120 °C for 4–168 h, broad diffractions at about 26° and 32° in 2θ were observed as indicated by solid circles, which corresponded to the diffractions from HAp. The other sharp diffractions in Fig. 1b–f agreed with those of LTA with Ca^{2+} replaced by NH_4^+, indicating that the cation sites in the Ca-LTA were occupied by NH_4^+ during the hydrothermal treatments as described by Matsumoto et al.[16] The XRD patterns demonstrated that there was no significant difference in the full-width at half maximum intensity (FWHM) before and

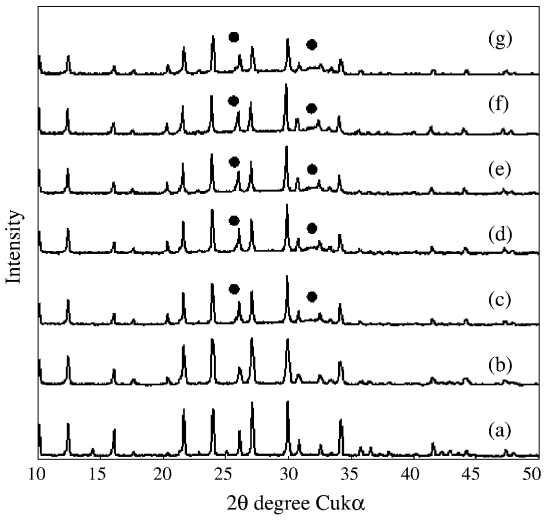

Fig. 1. XRD patterns of (a) Ca-LTA and LTAs after the hydrothermal treatments at 120 °C for (b) 1 h, (c) 4 h, (d) 8 h, (e) 24 h, (f) 72 h and (g) 168 h. All diffractions in (a) are attributed to Ca-LTA. The solid circles indicate the diffractions of HAp. The other diffractions in (b–g) are attributed to NH_4-LTA.

after the hydrothermal treatments until 72 h (Fig. 1c–e), but the shift of the diffractions of LTA with NH_4^+ (NH_4-LTA) and the increases of the FWHM were found at 168 h. The results of XRD indicate that the LTA structure is stable in a 1 M $(NH_4)_3PO_4$ solution heated at 120 °C until 72 h, however the LTA structure starts to deteriorate at 168 h. The HAp thin layers were formed on the LTA surface after 4 h. The cation exchange model of Ca-LTA in the $(NH_4)_3PO_4$ solution can be described as Eq. (1) and the yield of HAp after the hydrothermal treatments described as Eq. (2):

$$5Ca_6(Si_{12}Al_{12}O_{48})\cdot nH_2O + 18PO_4(NH_4)_3\cdot nH_2O + 6NH_4(OH) \rightarrow 3Ca_{10}(PO_4)_6(OH)_2 + 5(NH_4)_{12}(Si_{12}Al_{12}O_{48})\cdot nH_2O + mH_2O \quad (1)$$

$$\alpha = \frac{X}{0.324W} \quad (2)$$

If weight (W, g) of LTA reacts perfectly in the $(NH_4)_3PO_4$ solution, the theoretical increase of the weight is $0.324W$ g. Therefore, the yield, α, can be calculated by Eq. (2) using experimental data, where X is the weight increase of the formation of HAp at nominated durations and temperatures. Fig. 2 shows the change of the HAp yields after hydrothermal treatments of Ca-LTA at 120 °C against various durations. The increase of α at 4 h indicates the formation of HAp on the LTA surface, which was matched to the results of XRD measurements. The maximum value of α is 0.82 at 8 h, which is 20-fold larger than the value in the formation of HAp on alite.[12]

The compositions of Ca-LTAs before and after the reaction at 120 °C, analyzed with ICP-AES, were shown in Table 1. The Si/Al mole ratio was not changed to be near 1.0 before and after the reaction. The Ca/P mole ratio after the reaction was 1.69, which was matched to the theoretical Ca/P ratio of HAp. The yield (α) of HAp was calculated to be 0.79, which is almost equal to the result ($\alpha = 0.82$) calculated from the weight changes. On the contrary, at 168 h, the α value was decreased because the dissolution of cations caused the destruction of the LTA structure.

Table 1
The composition of Ca-LTA before and after the hydrothermal treatment at 120 °C

	Ca-LTA (10^{-4} mol)	HAp-LTA (10^{-4} mol)
Si	2.74	2.42
Al	2.74	2.37
Si/Al	1.00	1.02
Ca	1.30	0.91
P	N.D.	0.54
Ca/P		1.69

N.D.: not detected. HAp-LTA: Ca-LTA after the reaction at 120 °C.

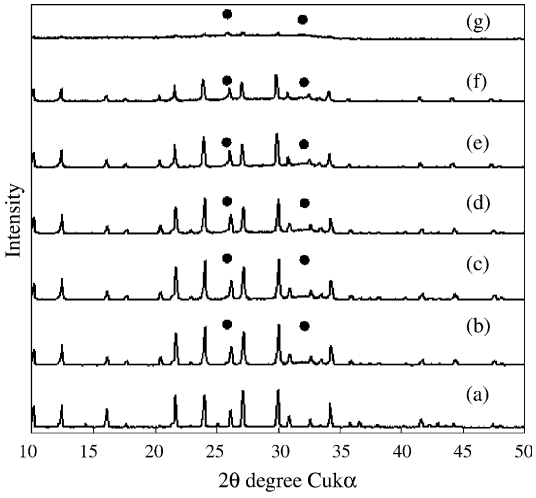

Fig. 3. XRD patterns of (a) Ca-LTA and LTAs after the hydrothermal treatment at (b) 25 °C, (c) 40 °C, (d) 80 °C, (e) 120 °C, (f) 160 °C and (g) 200 °C for 8 h. All diffractions in (a) are attributed to Ca-LTA. The black circles indicate the diffractions of HAp and the other diffractions in (b–g) are attributed to NH_4-LTA.

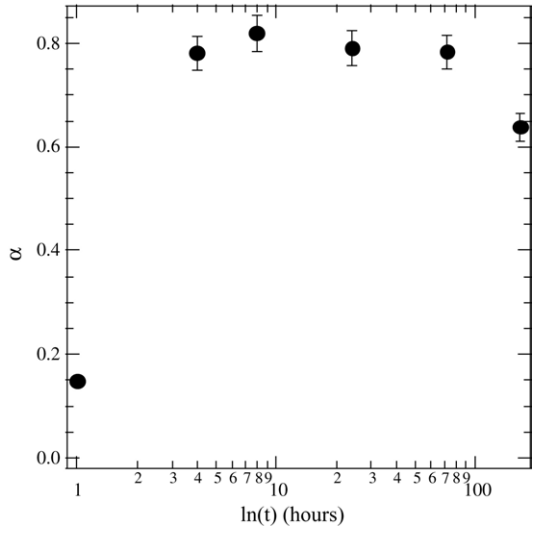

Fig. 2. The change of the HAp yields after hydrothermal treatment of Ca-LTA at 120 °C vs. various durations.

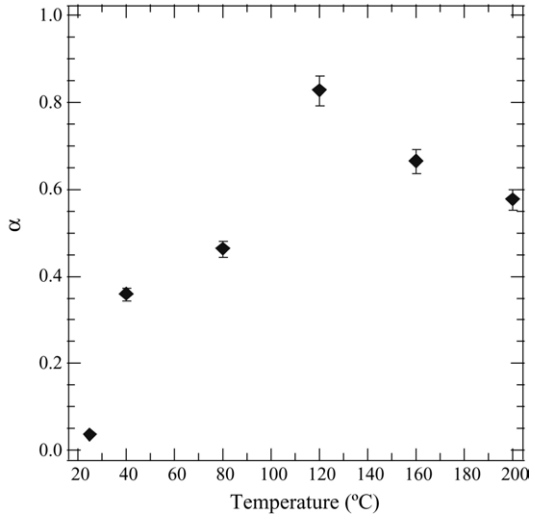

Fig. 4. The change of the HAp yields after the hydrothermal treatment of Ca-LTA for 8 h vs. the various temperatures.

Fig. 3 shows the XRD patterns of Ca-LTA before and after the hydrothermal treatments at 25–200 °C for 8 h. After the hydrothermal treatments, broad diffractions at about 26° and 32° in 2θ were observed as indicated by solid circles, which corresponded to the diffractions of HAp. The HAp crystals were grown at any synthetic temperature. The other sharp diffractions in Fig. 3b–f coincided with those of NH_4-LTA. These XRD patterns demonstrated that there was no significant difference in FWHM before and after the hydrothermal treatment at 25–160 °C, but a decrease of the diffraction intensity and an increase of FWHM were found at 200 °C. We thus conclude that the LTA structure is stable in the 1 M $(NH_4)_3PO_4$ solution heated at 25–160 °C for 8 h but the structure starts to deteriorate at 200 °C.

Fig. 4 shows the change of the HAp yields after the hydrothermal treatments of Ca-LTA for 8 h against the various temperatures. The α values increased against the temperature range of 25–120 °C but decrease against 160–200 °C. The increase of α values was attributed to the formation of HAp and the decrease was corresponded to the destruction of the LTA structure. The maximum α value at 120 °C showed the homogeneous covering of HAp on the surface of LTA as shown in the next SEM image.

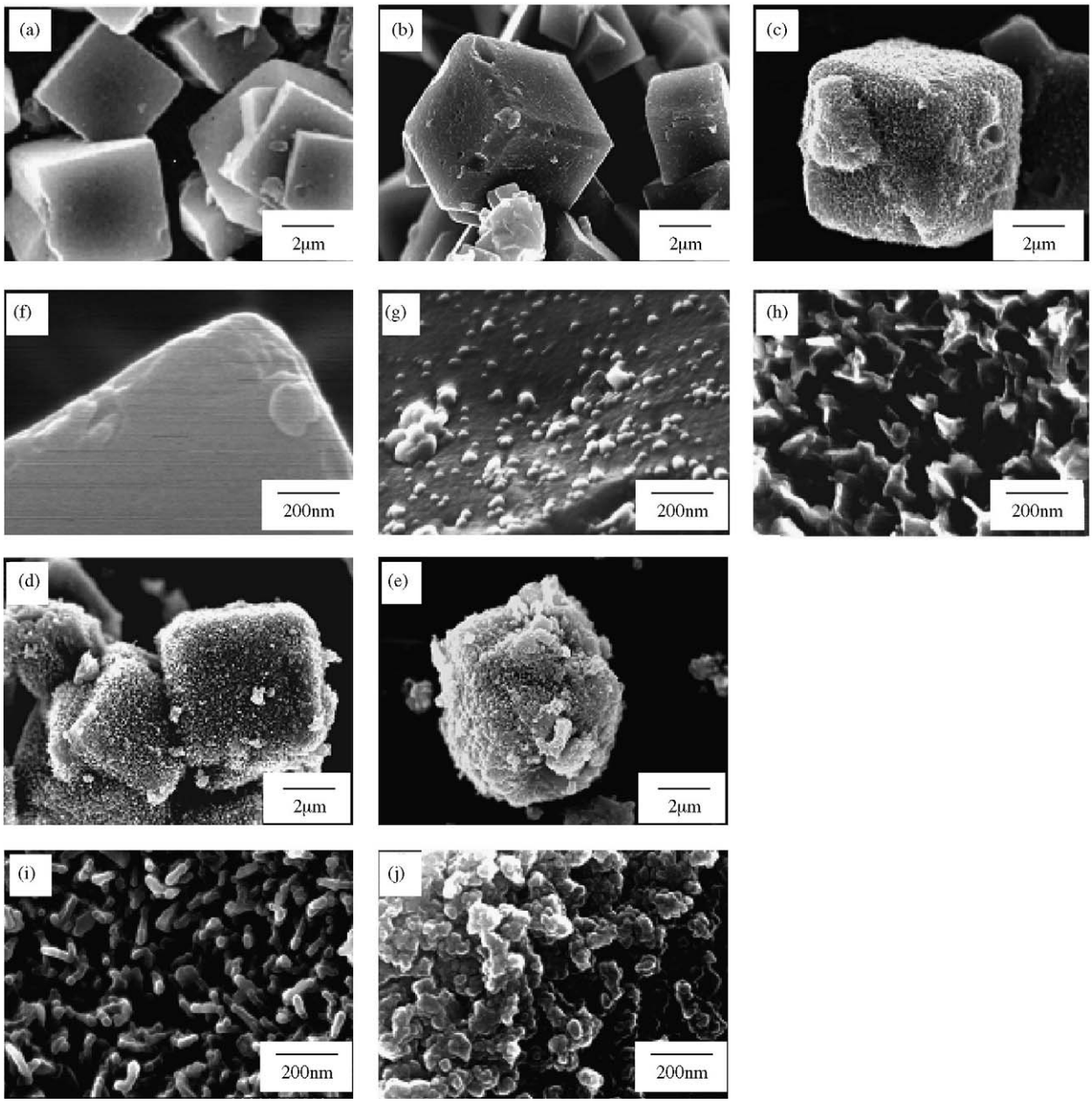

Fig. 5. SEM images of Ca-LTA (a and f) and LTAs after the hydrothermal treatment at various temperatures for 8 h; (b and g) 25 °C, (c and h) 40 °C, (d and i) 120 °C and (e and j) 200 °C.

Fig. 5 shows the SEM images of Ca-LTA and those after the hydrothermal treatments at 25–200 °C for 8 h. The morphology of the Ca-LTA before the treatments exhibited a cubic automorphism with smooth surface. The surface of the Ca-LTA heated at 25 °C was covered by tiny ball-like HAp particles with the sizes of about 30 nm in diameter (Fig. 5b and g). This morphology was very similar to that of HAp formed in SBF.[9–11] The morphology of the Ca-LTA at 40 °C showed tiny scaly HAp particles of about 80 nm in diameter (Fig. 5c and h). The Ca-LTA surface at 120 °C was covered by needle-like HAp crystals of 100–200 nm in diameter (Fig. 5d and i). The morphology was very similar to that of HAp formed under same hydrothermal treatment.[17] At 200 °C the amorphous-like particles were covered with the destroyed LTA (Fig. 5e and j), which corresponded with the XRD patterns shown in Fig. 3g.

TEM was applied to the observation of the interface between HAp and LTA. The TEM images as shown in Fig. 6 clearly indicated the HAp crystals of 30 nm in length grown on the LTA surface in the treatment at 40 °C, and the complete covering of needle-like HAp crystals of up to 100 nm in length in the treatment at 120 °C. In our previous study, the needle-like HAp crystals grew roughly perpendicular to the LTA surface from the SAED pattern.[13]

Moriyoshi et al.[12] have discussed a formation mechanism of HAp on alite. According to their report, Ca^{2+} in the structure of alite released into a $(NH_4)_3PO_4$ solution reacts very rapidly with PO_4^{3-} to form further HAp crystals. Liu et al.[10] have also reported a formation mechanism of HAp on wollastonite in a simulated body fluid (SBF). They discussed that Ca^{2+} released from wollastonite increase the ion activity of apatite in SBF, and hydrate silica on the surface of wollasonite provides the sites favorable for apatite nucleation. Consequently, the apatite nuclei are rapidly formed on the surface of wollastonite. The release of the Ca^{2+} was dependent on its solubility. However, in our study, the reaction of Ca-LTA with ammonium phosphate is the ion exchange model shown in Eq. (1). The exchange of Ca^{2+} on LTA for NH_4^+ in a $(NH_4)_3PO_4$ solution is a driving force of the formation of HAp, and then the discharged Ca^{2+} reacts with phosphate ions on the surface of LTA due to Ca supersaturation at local area. The reaction of HAp formation in the previous study was related to the amount of calcium dissolution from alite. For this reason, the yield (maximum $\alpha = 0.04$) for HAp formation is smaller than that (maximum $\alpha = 0.82$) of LTA in this study. Furthermore, these substrates were self-destroyed in the reactions to form HAp. In this study, however, the reaction of HAp formation occurred by ion exchange reaction following Eq. (1). In particular, this reaction is pronounced in an ammonium phosphate solution because of the high NH_4^+ selectivity of LTA. The Ca^{2+} ions in Ca-LTA were almost involved in the formation of HAp crystals on the surface of LTA.

Table 2
The specific surface areas of Ca-LTA and samples synthesized from 25 to 200 °C for 8 h

Samples	Specific surface area (m^2/g)
Ca-LTA	591.0
LTA25	548.6
LTA40	584.8
LTA80	223.5
LTA120	148.5
LTA160	128.9
LTA200	31.1

Ca-LTA treated at 25, 40, 80, 120, 160 and 200 °C are shown as LTA25, LTA40, LTA120, LTA160 and LTA200, respectively.

The specific surface areas of Ca-LTA and samples synthesized from 25 to 200 °C are shown in Table 2. The specific surface areas of samples synthesized at 25 and 40 °C for 8 h were almost the same as compared to that of Ca-LTA, and the pore diameter (0.88 nm) remains almost constant. These results mean that pores in LTA are completely maintained at the applied conditions. The prepared nanocomposites possess the combined adsorption characteristics of LTA and HAp. At hydrothermal treatment over 80 °C, the specific surface areas of samples decreased with increase of temperature. These results mean that the pores in LTA are partially covered by

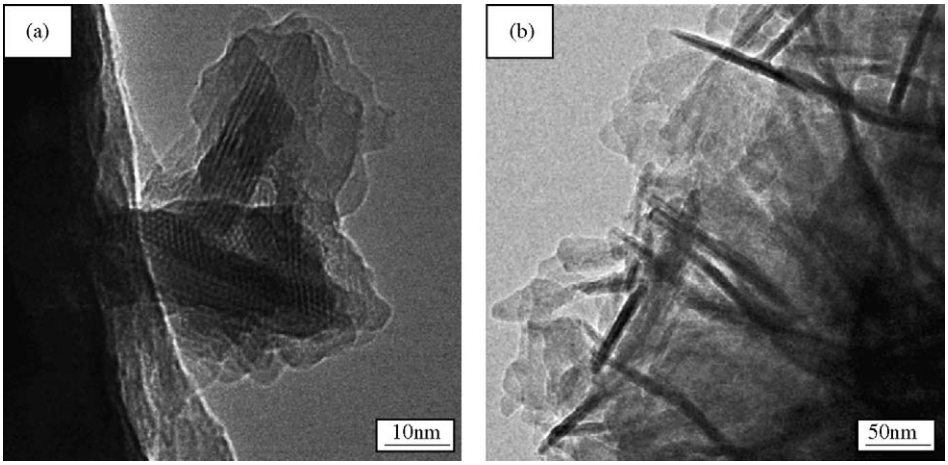

Fig. 6. The TEM images of Ca-LTA after the hydrothermal treatment at (a) 40 °C and (b) 120 °C for 8 h.

HAp thin layers. The materials are promising as material for encapsulate harmful ions or radioactive ion absorbed in LTA.

4. Conclusions

We successfully obtained the nanocomposite, HAp coated LTA by a new concept, which makes use of the intrinsic exchange properties of one of the starting compounds. The ion exchange of Ca^{2+} on LTA for NH_4^+ in an ammonium phosphate solution is a driving force for the formation. The structure of LTA was not destroyed by the hydrothermal treatment at 25–160 °C for 8 h and also at 120 °C for 1–72 h. The yield of LTA with HAp thin layers synthesized at 120 °C for 8 h showed maximum value of 0.82. The specific surface area was maintained in the treatment at 25 and 40 °C for 8 h as compared with that of Ca-LTA, but over 80 °C, the value decreased with an increase of temperature. These nanocomposites obtained are novel materials for the simultaneous adsorption and capsulation of both harmful and radioactive ions, possessing the excellent characteristics of both zeolite and hydroxyapatite.

Acknowledgements

A part of this study was financially supported by the Budget for Nuclear Research of the Ministry of Education, Culture, Sports, Science and Technology, based on the screening and counseling by the Atomic Energy Commission. We also wish to thank Mr. Y. Yajima for his help in ICP analysis.

References

1. Breck, D. W., In *Zeolite Molecular Sieves*, ed. D. W. Breck. Wiley, New York, 1974, pp. 1–185.
2. Meier, W. M., Olson, D. H. and Baerlocher, C., Atlas of zeolite structure types. *Zeolites*, 1996, **17**, 1–229.
3. Watanabe, Y., Yamada, H., Kokusen, H., Tanaka, J., Moriyoshi, Y. and Komatsu, Y., Ion exchange behavior of natural zeolites in distilled water, hydrochloric acid, and ammonium chloride solution. *Sep. Sci. Technol.*, 2003, **38**, 1519–1532.
4. Watanabe, Y., Yamada, H., Tanaka, J., Komatsu, Y. and Moriyoshi, Y., Ammonium ion exchange of synthetic zeolites: the effect of their open-window sizes, pore structures, and cation exchange capacities. *Sep. Sci. Technol.*, 2004, **39**, 2091–2104.
5. Watanabe, Y., Yamada, H., Kokusen, H., Tanaka, J., Moriyoshi, Y. and Komatsu, Y., Effect of cage-size on ammonium adsorption by synthetic zeolites. In *Proceedings of the 18th International Japan–Korea Seminar on Ceramics*, 2001, pp. 543–547.
6. Mimura, H. and Akiba, K., Adsorption behavior of cesium and strontium on synthetic Zeolite-P. *J. Nucl. Sci. Technol.*, 1993, **30**, 436–443.
7. Song, K. C., Lee, H. K., Moon, H. and Lee, K. J., Simultaneous removal of the radiotoxic nuclides Cs-137 and I-129 from aqueous solution. *Sep. Purif. Technol.*, 1997, **12**, 215–227.
8. Moreno, E. C., Kresak, M. and Zaharadnik, R. T., Fluoridated hydroxyapatite solubility and caries formation. *Nature*, 1974, **24**, 64–65.
9. Liu, X. Y. and Ding, C. X., Morphology of apatite formed on surface of wollastonite coating soaked in simulate body fluid. *Mater. Lett.*, 2002, **57**, 652–655.
10. Liu, X. Y., Ding, C. X. and Wang, Z. Y., Apatite formed on the surface of plasma-sprayed wollastonite coating immersed in simulated body fluid. *Biomaterials*, 2001, **22**, 2007–2012.
11. Siriphannon, P., Kameshima, Y., Yasumori, A., Okada, K. and Hayashi, S., Formation of hydroxyapatite on $CaSiO_3$ powders in simulated body fluid. *J. Eur. Ceram. Soc.*, 2002, **22**, 511–520.
12. Moriyoshi, Y., Chiba, H., Monma, H. and Ikegami, T., Preparation of hydroxyapatite in a reaction between alite and phosphoric acid. *Trans. Mater. Res. Soc. Jpn.*, 2002, **25**, 13–16.
13. Watanabe, Y., Moriyoshi, Y., Hashimoto, T., Suetsugu, Y., Ikoma, T., Kasama, T. *et al.*, Hydrothermal preparation of type-A zeolite with hydroxyapatite surface layers. *J. Am. Ceram. Soc.*, 2004, **87**, 1395–1397.
14. Watanabe, Y., Moriyoshi, Y., Hashimoto, T., Kasama, T., Suetsugu, Y., Ikoma, T. *et al.*, Characterization of type-A zeolite with hydroxyapatite surface layer prepared by hydrothermal treatment. In *Proceedings of the 20th International Japan–Korea Seminar on Ceramics*, 2003, pp. 213–216.
15. Breck, D. W., Eversole, W. G., Milton, R. M., Reed, T. B. and Thomas, T. L., Crystalline zeolites I. The properties of a new synthetic zeolite, type A. *J. Am. Chem. Soc.*, 1956, **78**, 5963–5971.
16. Matsumoto, T., Goto, Y. and Urabe, K., Formation process of mullite from NH_4^+-exchanged zeolite A. *J. Ceram. Soc. Jpn.*, 1995, **103**, 93–95.
17. Fujishiro, Y., Yabuki, H., Kawamura, K., Sato, T. and Okuwaki, A., Preparation of needle-like hydroxyapatite by homogeneous precipitation under hydrothermal conditions. *J. Chem. Technol. Biotechnol.*, 1993, **57**, 349–353.